An Infrared and Theoretical Study about the "XCN" Band Formation: Reactivity of HNCO with NH_3 Astrophysical Ice Laboratory Analogues and the Spontaneous Production of OCN^-

Sébastien Raunier, Thierry Chiavassa, Francis Marinelli, Alain Allouche, and Jean-Pierre Aycard*

Physique des Interactions Ioniques et Moléculaires, Equipe Spectrométries et Dynamique moléculaire, UMR 6633, Université de Provence, Centre de Saint Jérôme, Boite 252, F-13397 Marseille Cedex 20, France

Received: June 23, 2003; In Final Form: September 2, 2003

The reactivity of HNCO with molecular NH_3 and with NH_3 ices is investigated between 10 and 150 K with use of FT-IR spectroscopy and ab initio calculations. In argon matrix at 10 K, the formation of a 1/1 molecular complex between HNCO and NH_3 is observed. Its structure determined by DFT calculations at the B3LYP/6-31G(d,p) level exhibits a strong hydrogen bond (1.825 Å) between the hydrogen donor (HNCO) and NH_3. The warming up between 10 and 150 K of adsorbed HNCO on crystalline and on amorphous NH_3 ices shows the formation of $NH_4^+OCN^-$ at 50 and 90 K, respectively. These results are different from the ones obtained when HNCO is embedded in a NH_3 matrix. In this case, spontaneous formation of $NH_4^+OCN^-$ is observed at 10 K. Quantum calculations confirm this spontaneous character of the reaction. It occurs if HNCO is in an environment of four NH_3 and if one of them is directly in interaction with HNCO via its electron lone pair. The crystal NH_3 unit cell parameters were optimized by using theoretical calculations (DFT method combined with a plane wave basis set and nonlocal reciprocal space pseudopotential) and used in the cluster model representing the ice surface. Absorption energy of HNCO on the NH_3 ice surface (−74.3 kJ/mol) is obtained with use of the DFT set. For the energy minimum, the cluster surface is modified and shows a strong hydrogen bond (1.662 Å) between the hydrogen of HNCO and a N atom of the surface as observed in argon matrix. HNCO lies flat on the surface and the oxygen of HNCO interacts with another neighboring NH group.

1. Introduction

Up to now, more than 100 interstellar molecules have been identified in the interstellar medium.[1] Many of these molecules result from an efficient accretion reaction of atoms and molecules from gas on icy dust grains in the dense molecular clouds.[2] The composition of interstellar ices is revealed by infrared spectroscopy of protostellar sources. They should contain many of the species seen in the gas phase and new compounds resulting from thermal or photochemical reactions. Hydrogen is 3 to 4 orders of magnitude more abundant than the most reactive heavier elements, and grain surface chemistry is largely moderated by the local H/H_2 ratio. Thus, two qualitatively different types of ice mantle may be produced by surface reactions of these grains, hydrogen rich ices (polar ices) dominated by H_2O ice with CH_4 and NH_3, and other hydrogen poor ices (apolar ices) composed of molecules such as CO, CO_2, O_2, and N_2.[3]

Since its discovery in 1979 by Soifer et al.[4] in the protostar W33A, the 4.62 μm (2167 cm^{-1}) feature has been extensively sought[5] and numerous carriers, such as nitriles[6] and isonitriles,[7] have been proposed for this absorption band called "XCN". Its position and width led to assigning it to a solid molecular species. In 1987, Grim and Greenberg[8] discussed the spectroscopy validity of the "XCN" band assignment to nitriles and isonitriles. They proposed the identification of the "XCN" feature as the intense asymmetric stretch of the isocyanate anion (OCN^-). This attribution was confirmed later by Schutte and Greenberg[9] and more recently by Demyk et al.,[10] who detected three other bands of OCN^- at 1296, 1206, and 630 cm^{-1}. The "XCN" band is easily obtained during the photolysis of polar interstellar ice analogues containing $H_2O/CH_3OH/CO/NH_3$.[11] Hudson and Moore[12] confirm, from laboratory experiments on irradiated ices, and Novozamsky et al.,[13] from the study of the effects of different molecules on its behavior,[14] that the band produced is due to OCN^-. Grim and Greenberg[8] proposed that the formation of OCN^- is preceded by photochemical formation of isocyanic acid, HNCO, followed by proton transfer to some base such as NH_3. However, HNCO has been detected in the interstellar medium in the gas phase but never in the cold (10−100 K) interstellar grains.[15] In a previous work, we have studied the reactivity of isocyanic acid on the surface or in the bulk of pure water ice.[16] Our results showed that HNCO adsorbed on the dangling oxygen sites of water ice yields OCN^- only near 130 K. This result is different than the one observed with HNCO embedded in a NH_3 matrix.[17] In this latter case, acid−base reaction yielding OCN^- formation occurs at 10 K.

In this paper, we are interested in studying the reactivity of isocyanic acid with NH_3 ice analogues. NH_3 has been detected in different sources, based on observations of the inversion mode near 9.0 μm (1110 cm^{-1}) and the stretching mode at 2.95 μm (3390 cm^{-1}).[18] NH_3 abundance in astrophysical ices toward infrared sources is generally found around 10−15% relative to H_2O.[18] This suggests that gas−grains interactions may be important in the ammonia chemistry of molecular clouds. The purpose of the present work is 3-fold: (1) to obtain direct and accurate experiment results on the $HNCO-NH_3$ complexes

* Corresponding author. E-mail address: aycard@piimsdm3.univ-mrs.fr.

10.1021/jp035770m CCC: $25.00
Published on Web 10/11/2003

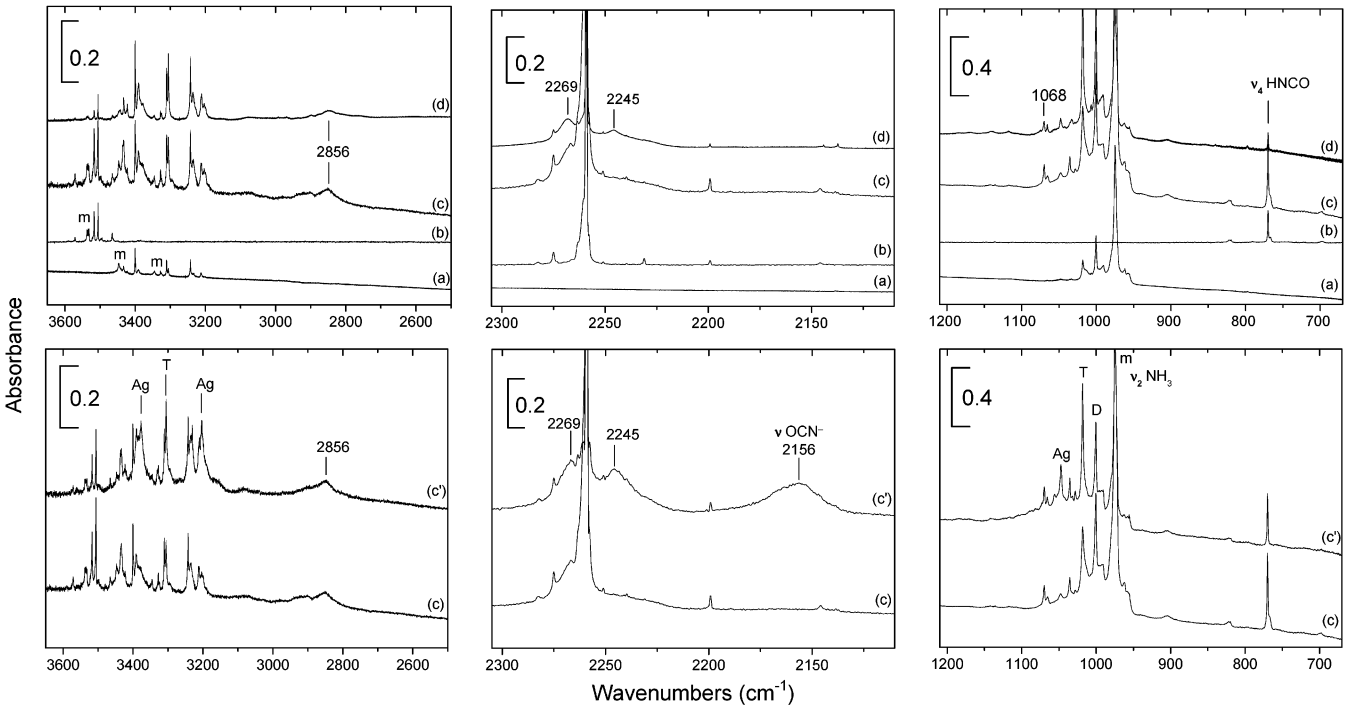

Figure 1. Spectra at 10 K: (a) NH_3/Ar 1/100; (b) HNCO/Ar 1/700; (c) HNCO/NH_3/Ar 2/2/1000; (d) HNCO/NH_3/Ar 2/20/1000. (c′) Annealing of HNCO/NH_3/Ar 2/2/1000 between 10 and 30 K.

trapped in rare gas cryogenic matrix; (2) to assess the chemical stability of HNCO adsorbed on amorphous and crystal NH_3 ice surfaces; and (3) to understand the reactivity of HNCO and the formation path of OCN^- in interstellar conditions.

Experiments were monitored by FT-IR spectroscopy. Quantum calculations were undertaken to compare the experimental IR spectra with the calculated ones and to model the NH_3 crystal surface. They also allow us to assign observed absorptions, to determine the complex geometry and the adsorption site structures, and furthermore to model the reactivity of HNCO on ice surfaces.

2. Experimental Section

Pure isocyanic acid was synthesized from thermal decomposition of cyanuric acid supplied by Aldrich Chemical (98%) at 650°C under primary vacuum, following the method described by Herzberg[19] and modified by Sheludyakov.[20] HNCO is trapped and conserved in a tube cooled by liquid nitrogen. The HNCO is degassed before each deposition. Moreover, the first fraction of isocyanic acid is evacuated. NH_3 is supplied by Air liquide (N 36, $H_2O \leq 200$ ppm) and ND_3 by Aldrich (99%). The concentration was estimated from standard manometric techniques. The apparatus and experimental techniques used to obtain argon matrices have been described elsewhere in the literature.[21] To study the reactivity of HNCO with NH_3, two separate inlets were used[17] to deposit the samples onto a gold-plated mirror under a constant pressure of 10^{-7} mbar. Previous to our study, we undertook, under the same conditions, a study of pure HNCO and pure NH_3 in an argon matrix and solid film by infrared spectroscopy. The infrared spectra were recorded with a FTIR spectrometer (Nicolet series II Magna 750) in the range 4000−500 cm^{-1} with a resolution of 0.125 and 0.5 cm^{-1} for respectively matrix and solid films. For each spectrum, 100 scans were collected. The thermal activation of the different samples was achieved through gradual warming up of the mirror from 10 K to the complete sublimation of the compounds, and using a heating rate of 1 deg/min for solid samples and 0.5 deg/min for annealing matrix samples.

2.1. Formation of HNCO−NH_3 Complexes: Cryogenic Matrix Experiments. Prior to this HNCO adsorption study on NH_3 ice surfaces, previous experiments were carried out in argon matrices to identify the structures of the HNCO−NH_3 complexes. Argon matrices containing only HNCO or NH_3 (ND_3) were prepared yielding infrared absorptions similar to those previously reported in the literature. The observed vibration bands are reported in Figure 1 and Table 1 with spectral assignment from the works of Sefik and Nishiya for NH_3[22] (Shimamouchi[22c] for ND_3) and Teles for HNCO.[23] These experiments were conducted with different compound concentrations to identify the characteristic absorption bands of free and multimer compounds.

The spectra recorded after co-deposition of Ar/NH_3 (500/2) and Ar/HNCO (500/2) mixtures at 10 K show new absorption bands with respect to the spectra of the pure compounds.

In the 3000−2800 cm^{-1} region relative to the ν_{NH} stretching, a new broad and weak absorption band (Figure 1c and Table 1) appears centered at 2856 cm^{-1} with respect to the spectra of the pure free compounds. This feature is shifted to low frequencies compared with the values expected for the ν_{NH} stretching of HNCO and NH_3 and it suggests the existence of a strong 1/1 hydrogen-bonded complex between HNCO and NH_3. This band is well correlated with the band at 2269 cm^{-1} located near the ν_{NCO} mode of HNCO monomer at 2259 cm^{-1}. Another band at 1068 cm^{-1} is also observed in the ν_2 region relative to the most intense band of NH_3, which is upshifted compared with the NH_3 monomer at 974 cm^{-1}. When a highest NH_3 concentration is used in the mixture (Ar/NH_3 (500/20) and Ar/HNCO (500/2)), in addition to the vibrational bands mentioned above, a new vibrational band can be unambiguously observed at 2245 cm^{-1} shifted to low frequency with respect to the ν_{NCO} mode of monomer HNCO (Figure 1d). At the same time, the absorption band intensities of NH_3 dimer (D), trimer

TABLE 1: Experimental and Calculated Frequency Shifts (cm^{-1}) of HNCO in $HNCO:NH_3$ and in $HNCO:ND_3$ 1:1 Complex with B3LYP/6-31G(d,p) ($\Delta\nu = \nu_{complex} - \nu_{monomer}$)

				1:1 complex					
		monomer		exper ment		calculation			
species	modes	ν_{exp}	ν_{calc}	ν_{exp}	$\Delta\nu_{exp}$	ν_{calc}	$\Delta\nu_{calc}$	int %	assignments
ND_3	ν_3	2564	2614			2654	40.0	0.0	ν_{NH}
	ν_1	2420	2466			2485	19.0	0.0	ν_{NH}
	ν_4	1191	1222			1220	−2.0	0.6	δ_{HNH}
	ν_2	748	814	830	82	871	57.0	4.6	δ_{HNH} (umbrella)
NH_3	ν_3	3587	3587			3606	19.0	0.4	ν_{NH}
	ν_1	3345	3460			3478	18.0	0.0	ν_{NH}
	ν_4	1638	1694			1683	−11.0	1.0	δ_{HNH}
	ν_2	974	1090	1068	94	1141	51.0	5.9	δ_{HNH} (umbrella)
HNCO	ν_1	3512	3701.2	2856	−655.5	3122.8	−578.4	100.0	ν_{NH}
	ν_2	2259	2356.6	2269	10	2360.6	4.0	28.0	ν_{NCO} (asym)
	ν_3		1338.7			1339.6	0.9	2.2	ν_{NCO} (sym)
	ν_4	770	792.0			1013.2	221.2	14.5	δ_{HNC}
	ν_5	573	559.4			580.6	21.2	3.1	oop_{NCO}
	ν_6	697	610.5			638.5	28.0	0.2	δ_{NCO}

(T), and aggregates (Ag) are highest in relative proportion with respect to those monomers obtained in the first experiment. An annealing at 30 K of the $Ar/NH_3/HNCO$ (1000/2/2) matrix induces similar effects to those obtained from a mixture containing a high concentration in NH_3. As previously observed, we observe an increase of the NH_3 multimer bands correlated with a decrease of those of free ammonia and the 2245 cm^{-1} feature is once more observed. This evolution is indicative of a NH_3 diffusion process during the matrix warming. This is responsible for formation of a new complex that could be a 1:2 complex ($HNCO:(NH_3)_2$) marked by the vibrational band at 2245 cm^{-1}. However, we do not detect in explanation of its very weak intensity, other vibrational bands in the ν_{NH} region of HNCO for this complex. During the annealing experiments, between 10 and 30 K, another band at 2157 cm^{-1} also appeared, which is in good agreement with the values expected for the antisymmetric stretching mode of the OCN^- ion. This last band suggests that a reaction between HNCO and NH_3 occurs leading to NH_4^+ and OCN^- ions. Nevertheless, we cannot identify features relative to the NH_4^+ ion because they are too weak. Above 45 K, argon sublimation induces the formation of solid $NH_4^+OCN^-$, which we have characterized in a previous paper.[17]

To unambiguously identify these complexes, we carried out isotopic experiments involving ND_3 instead of NH_3 molecules in the matrix mixtures at the same concentrations as in the previous experiments. All the vibrational bands of monomer and complexed HNCO are observed at the same frequencies and only the vibrational bands relative to ammonia are affected by the isotopic exchange. These latter are reported in Table 1. As previously observed, the ν_2 mode of ND_3 ammonia in the 1:1 complex is upshifted by 82 cm^{-1} and this value is very close to that recorded for the 1:1 $HNCO:NH_3$ complex. To help us with the assignment of these new bands, along with the experimental data on the monomers in matrices, we calculated further the vibrational spectra of the complex species using the optimized complex structures.

Considering the previous results obtained in argon matrices, we have studied the thermal behavior of HNCO molecules embedded in the ice bulk or adsorbed on NH_3 ice surfaces.

2.2. Infrared Spectra of NH_3 Ices. Staats and Morgan[24] have found that solid NH_3 can exhibit two metastable phases as well as the cubic structure phase. In 1980, Ferraro et al.[25] concluded the existence of only three phases: the stable cubic phase, an amorphous phase at 20 K, and a metastable phase at an intermediate temperature (50 K). Pipes et al.[26] then Mantz et al.[27] have recorded the infrared spectra of solid NH_3. Its spectrum is characterized by four fundamental modes noted ν_1 to ν_4 at 3210, 1075, 3375, and 1625 cm^{-1}, respectively, and at 530 cm^{-1} by the lattice band ν_5.

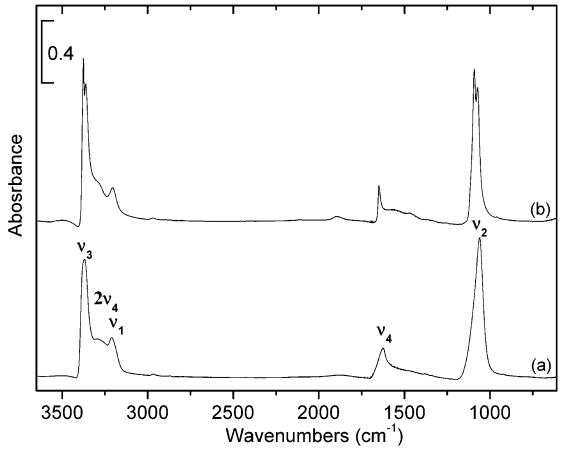

Figure 2. IR spectra of solid NH_3: (a) amorphous at 20 K and (b) cubic at 110 K.

At 20 K, the NH_3 ice obtained by spraying ammonia on a cold gold surface is an amorphous solid. In its infrared spectrum, the lattice band (ν_5) is not present and the fundamental bands are broad. Under our experimental conditions, warming of the bare ice between 20 and 110 K (1 deg/min) induces the phase transition to the crystalline phase ca. 70 K at 10^{-7} mbar. The infrared spectrum of this phase is characterized by a splitting of the ν_3 and ν_2 modes (3362, 3381 and 1100, 1075 cm^{-1} respectively (Figure 2 and Table 2) and an increasing of band intensities. X-ray study of solid ammonia[28] at −102 °C shows that each NH_3 molecule is involved in six hydrogen bonds, ruling out the possibility of dangling lone pair at the surface. Above 120 K, ammonia sublimates.

2.2.1. Co-deposition Experiments. When HNCO and an excess of NH_3 are co-deposited at 10 K (1/10 mixture), the HNCO IR spectrum shows three bands which are slightly shifted compared with the values observed for the solid HNCO[29] or HNCO embedded in the water environnement.[16] Regarding NH_3, the infrared spectra of solid HNCO at low temperature (10−45 K) has already been reported.[29] The solid HNCO IR spectrum is characterized by an intense vibrational band located at 2252 cm^{-1} and a broad feature split into two bands at 3245−3365 cm^{-1}, which are relative to the ν_{asNCO} and the ν_{NH} stretching modes (Table 3).

TABLE 2: Vibrational Modes of Solid NH_3 in the Amorphous (20 K) and Crystalline Phase (110 K)

	amorphous (20 K)		crystalline (110 K)	
modes	*a*	*b*	*a*	*b*
ν_2	1075	1071	1057 1100	1075 1100
ν_4	1625	1628	1490 1592 1620 1650	1459 1567 ? 1650
$2\nu_4$	3290	3287	3280	3291
ν_1	3210	3211	3210	3211
ν_3	3375	3373	3367 3374	3362 3381

[a] Ferraro et al.[25] [b] Our work.

TABLE 3: Experimental Frequencies (cm^{-1}) of HNCO Solid in H_2O and in NH_3 Environments at 10 K

modes	assignments	HNCO solid at 10 K	HNCO in H_2O solid at 10 K[16]	HNCO in NH_3 solid at 10 K
ν_1[a]	NH stretch	3365−3245		3218
ν_2	NCO asym stretch	2252	2242	2259
ν_3[b]	NCO sym stretch	1322−1252	1321−1261	1313−1254
ν_4	HNC bend	862		
ν_5	NCO in-plane bend	597		
ν_6	NCO out-of-plane bend	657		

[a] Two components are observed for this mode. Such a splitting is due to hydrogen bond interaction. [b] Fermi resonance of ν_3 and $2\nu_6$.

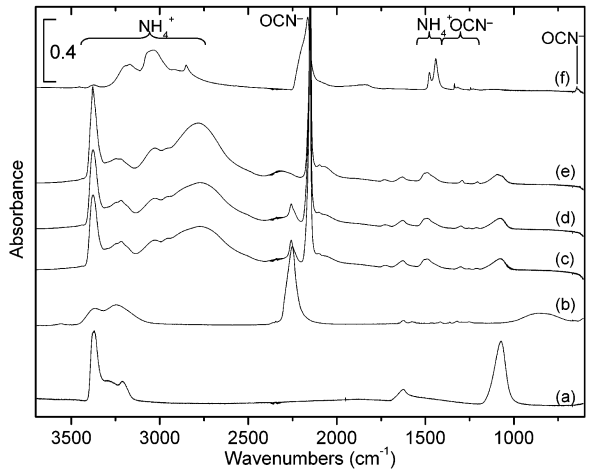

Figure 3. $HNCO/NH_3$ co-deposition experiments (ratio 1/10): (a) pure NH_3 at 10 K; (b) pure HNCO at 10 K; (c) $HNCO/NH_3$ at 10 K; (d) at 30 K; (e) at 120 K; and (f) at 160 K.

The most prominent spectral feature in the mixture is that due to the spontaneous formation of $NH_4^+OCN^-$ due to an acid base reaction in the bulk between the two moieties (Figure 3). The $NH_4^+OCN^-$ absorption bands are reported in Table 4 with their assignments. The OCN^- ion is characterized by an intense band at 2151 cm^{-1} and by two weaker bands at 1212 and 630 cm^{-1} relative to the asymmetric stretching and the symmetric bending modes,[9] respectively. We can point out that the ν_{asOCN^-} frequency (2151 cm^{-1}) is different from that observed in a H_2O environment (2170 cm^{-1})[16] or in an argon matrix (2157 cm^{-1}). NH_4^+ is characterized by a weak absorption band at 1495 cm^{-1} assigned to the NH bending and by a broad and intense band in the region near 2700 cm^{-1}, which is the superposition of NH stretch and combination modes.[30] During the warming process, we observe at 30 K, due to a possible NH_3 diffusion

TABLE 4: Experimental Frequencies (cm^{-1}) of $NH_4^+OCN^-$ at 10 K in NH_3 Environment and $NH_4^+OCN^-$ Solid at 160 K

	modes	assignments	$NH_4^+OCN^-$ in solid NH_3 at 10 K	$NH_4^+OCN^-$ solid at 160 K
NH_4^+	$\nu_1+\nu_5$	combination mode	3225	3200
	ν_3	NH stretch		3170
	$\nu_2+\nu_4$	combination mode	3030	3034
	$2\nu_4$	1st overtone of NH bend	2800	2853
	$\nu_2+\nu_6$	combination mode	2080	2080
	ν_2	NH bend	1630	
	ν_4	NH bend	1495	1477−1441[a]
OCN^-	ν_3	OCN asym stretch	2151	2165
	$2\nu_2$	1st overtone of OCN bend	1300	1335−1317[a]
	ν_1	OCN sym stretch	1212	1244−1227[a]
	ν_2	OCN bend	630	645

[a] Splitting probably due to a crystallization effect.

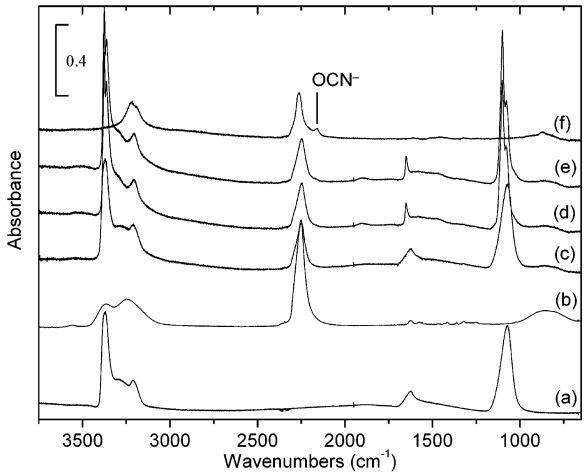

Figure 4. Adsorption of HNCO on NH_3 surface: (a) NH_3 at 10 K; (b) HNCO at 10 K; (c) HNCO on NH_3 at 10 K; (d) at 70 K; (e) at 90 K; and (f) at 130 K after sublimation of NH_3.

in the mixture, a decrease of the HNCO bands and an increase of the $NH_4^+OCN^-$ ones. This result indicates that the $NH_4^+OCN^-$ formation continues up to 120 K with unreacted HNCO in the solid (Figure 3). After complete sublimation of NH_3 at 125 K, we observe only $NH_4^+OCN^-$, which displays an IR spectrum quite different from the one recorded at 10 K (Figure 3 and Table 4). This vibrational change shows that NH_3 significantly disturbs the $NH_4^+OCN^-$ surroundings. In its crystalline form, $NH_4^+OCN^-$ displays the NH_4^+ cation surrounded by eight OCN^- anions.[31] After residual HNCO sublimation at 160 K, the ν_{asOCN^-} frequency appears at 2165 cm^{-1}, a value similar to the one obtained by Bernstein et al.[32] from CO/NH_3 ice irradiation experiments.

2.2.2. Adsorption on NH_3 Ice Surfaces. No reaction occurs when HNCO is adsorbed on amorphous NH_3 ice at 10 K. In the infrared spectra the ν_{NCO} band is shifted to low frequency by 5 cm^{-1}, and appears at 2248 cm^{-1}. Warming up the sample to 90 K induces the phase transformation of amorphous NH_3 ice to crystalline NH_3 and the apparition of a new weak band at 2163 cm^{-1} assigned to the ν_{asOCN^-} stretching mode. After complete NH_3 sublimation at 125 K, the IR spectrum shows features similar to those observed for $NH_4^+OCN^-$ in the co-deposition experiment (Figure 4).

Since no reaction occurs at 10 K, but only when HNCO is co-deposited with NH_3, we suggest a solvation-induced dissociative ionization process. To confirm this hypothesis, we performed calculations on HNCO ionization in direct interaction with NH_3 molecules.

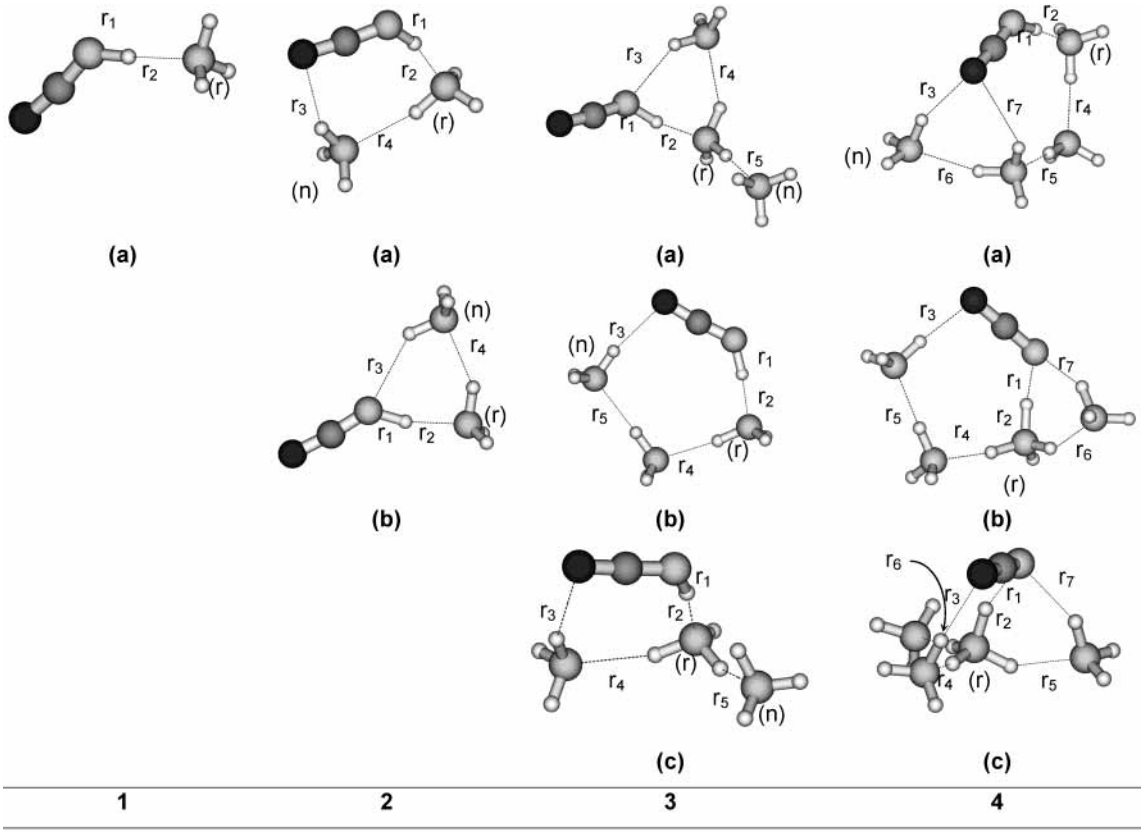

Figure 5. Different optimized HNCO:$(NH_3)_n$ clusters with $n = 1-4$, carried out with B3LYP/6-31G(d,p).

When HNCO is directly adsorbed on crystalline bare NH_3 ice at 10 K, the ν_{NCO} band appears at 2254 cm^{-1} and is upshifted compared with the value observed for HNCO on NH_3 amorphous ice. Then the sample is warmed up, with the same heating rate used in the previous experiment, from 10 to 200 K. The absorption band of the OCN^- species at 2165 cm^{-1} appears at 50 K. The reaction between HNCO and NH_3 goes until ammonia sublimates above 130 K; then unreacted HNCO sublimates at 160 K. The IR spectrum recorded at 200 K shows only the $NH_4^+OCN^-$ absorption bands as displayed in Figure 3f.

3. Computational Results

3.1. Complex Structures and Formation of OCN^-. We have carried out quantum calculations to explain our experimental observations. These calculations show that the diffusion of NH_3 in an argon matrix plays an important role on the OCN^- formation. To establish the molecular structure observed in matrix experiments, ab initio calculations were carried out with Gaussian 98.[33] The different systems were optimized at the B3LYP/6-31G(d,p) level of theory[34] and are noted as HNCO-$(NH_3)_n$ ($n = 1-4$). The interaction energy of these systems, ΔE, was calculated by using the following equation:

$$\Delta E_{BSSE}(n) = E^{Tot}_{BSSE}[HNCO(NH_3)_n] - E_{BSSE}[HNCO] - E_{BSSE}[(NH_3)_n]$$

Each term is calculated using the entire orbital set as usual in the Boys counterpoise method (BSSE correction).[35]

3.1.1. Complex Structure. The determination of the complex structure corresponds to the system HNCO$(NH_3)_n$ with $n = 1$. Considering the properties of NH_3, several arrangements of the complex subunits are possible and different kinds of complexes are expected. Hence, the electron lone pair of NH_3 is considered to attack HNCO on the acid hydrogen or on the carbon atom. Moreover, possibilities of hydrogen bonds between NH_3 hydrogen and isocyanic oxygen were examined. Calculation results yield only one local minimum.

The obtained structure features a strong hydrogen bond (H-bond) ($r_2 = 1.825$ Å in 1(a) in Figure 5) between the hydrogen of HNCO and the nitrogen of NH_3, forming an angle (N−H···N) of 177.2°. The stabilizing energy of the system is −46 kJ/mol. In this configuration, HNCO displays a proton donor character and the covalent bond length NH (r_1) of HNCO (H−NCO) is 1.040 Å (1.008 Å for isolated HNCO). We call this first NH_3 the reactive NH_3 molecule in our next study and we note it NH_3(r).

These calculations provide valuable insight into the stability and the spectroscopic features of the complexes. The complexing effect can be observed on the geometry of the partner molecules and on their most significant stretching frequencies. To confirm the presence of this form in argon matrices, we have compared the experimental frequency shifts of the complex with those calculated for the free moieties (Table 1).

In the case of the 1/1 complex, we observe a good agreement between the calculated and experimental HNCO and NH_3 mode frequency shifts which are predicted as the most intense bands. In the spectrum, the ν_1 and ν_2 modes of HNCO are respectively shifted by −655.5 and +10 cm^{-1} experimentally against −578.4 and +4 cm^{-1} theoretically. A shift by 221.2 cm^{-1} is predicted on the ν_4 mode of HNCO, which is expected to be intense. However, this band cannot be observed because it falls in the ν_2 mode region of NH_3 near 1000 cm^{-1}. This observation is similar with ND_3, in the ν_4 mode region. Despite the prediction that the calculated vibrational mode of HNCO ν_1 should be the most intense, experimentally ν_1 is found to be weaker than the HNCO ν_2 mode. This effect could be understood in terms of the noncalculated effect of the relaxation along the hydrogen

TABLE 5: Different Parameters for HNCO:$(NH_3)_n$ Clusters ($n = 1-4$)[a]

NH_3	first	second		third			fourth		
structure	1(a)	2(a)	2(b)	3(a)	3(b)	3(c)	4(a)	4(b)	4(c)
r_1	1.040	1.061	1.060	1.088	1.064	1.101	1.087	1.551	1.715
r_2	1.825	1.730	1.721	1.617	1.665	1.584	1.611	1.108	1.070
r_3		2.489	2.405	2.366	2.192	2.544	2.208	2.003	2.046
r_4		2.101	2.070	2.169	2.022	2.153	1.930	1.781	1.892
r_5				2.094	2.143	2.161	2.014	1.979	1.952
r_6							2.136	1.930	1.945
r_7							2.664	2.170	2.137
ΔE(BSSE)	−46.14	−64.79	−67.46	−89.03	−89.45	−90.70	−99.48	−375.30	−453.18

[a] r_1 to r_7 given in Å and interaction energies ΔE(BSSE) given in kJ/mol.

bond which is existing between HNCO and NH_3. Indeed, the calculation we have carried out does not take into account this above-mentioned effect. Moreover, this effect is well-known to induce a broadening (over hundreds of wavenumbers) such as that we observe for the HNCO ν_1 mode. For NH_3, the ν_2 mode appears at 1068 cm^{-1} upshifted by 94 cm^{-1} compared to the respective monomer mode whereas a significant shift by 51 cm^{-1} is calculated. The band observed at 830 cm^{-1} confirms a shift of the ND_3 ν_2 mode of +82 cm^{-1} experimentally against +57 cm^{-1} theoretically.

3.1.2. Formation of $NH_4^+OCN^-$. To explain the spontaneous formation of $NH_4^+OCN^-$ observed in our co-deposition and in the diffusion of ammonia in matrix experiments, we modeled the interaction between HNCO and $n$$NH_3$ molecules ($n = 2-4$ in HNCO:$(NH_3)_n$). We added a new NH_3 molecule, noted as NH_3(n), to the previous complex structure HNCO(NH_3). The adding position of the new NH_3 to the system is important to model two effects: (1) the solvation effect on NH_3(r) by addition of NH_3 molecules in interaction with its free hydrogen and (2) the bulk effect of HNCO by addition of NH_3 molecules in interaction with the oxygen of HNCO.

The parameters of the different optimized structures are reported in Figure 5 and Table 5.

(i) $n = 2$: For two NH_3 molecules interacting in the system, we obtained two optimized structures noted as **2(a)** and **2(b)**, which present three H-bonds forming quasiplanar cycle:

(1) The first **2(a)**, the less stable (ΔE(BSSE) = −64.79 kJ/mol), exhibits the first H-bond between the H of HNCO and the nitrogen of the NH_3(r) ($r_2 = 1.730$ Å). The second H-bond between one hydrogen of NH_3(r) and the nitrogen of the additional NH_3 ($r_4 = 2.101$ Å) corresponds to the NH_3 dimer interaction. The last H-bond is between the oxygen of HNCO and the hydrogen of the adding NH_3 ($r_3 = 2.489$ Å) noted NH_3(n).

(2) The second configuration is the most stable (ΔE(BSSE) = −67.46 kJ/mol). In this case, HNCO serve as both the proton donor to the NH_3(r) and the proton acceptor by its electron lone pair with NH_3(n). The r_2 distance, 1.721 Å, is shorter, indicating a strong reinforcement of the hydrogen bond. Simultaneously, r_1 very slightly increases to 1.060 Å and the r_3 value, between the N of HNCO and H of NH_3(n), is 2.405 Å. This value denotes a rather weak H-bond. The bond length (r_4) between the two NH_3's is 2.070 Å.

The energy gain between **1(a)** and **2(a)** is about −18 and that between **1(a)** and **2(b)** is −21 kJ/mol. Adding extra solvent molecules reinforces r_2 (1.825−1.730 Å for **2(a)** and 1.825−1.721 Å for **2(b)**). One consequence is to weaken the involved covalent bond ($r_1 = 1.040-1.060$ Å for **2(a)** and **2(b)**) as already has been frequently reported.[36]

For these systems, the calculations predict that the frequencies of the HNCO ν_2 mode at 2338.6 and 2350.8 cm^{-1} respectively for **2(a)** and **2(b)** are shifted by −17.9 and −5.8 cm^{-1}, respectively, with respect to the monomer ν_2 frequency. Experimentally, these shifts are consistent with that observed for the HNCO$(NH_3)_2$ complex marked with only one band located at 2245 cm^{-1}, and shifted by −14 cm^{-1} compared with the monomer ν_2 value. However, the nondetection of the other bands for this complex does not allow an attribution to **2(a)** or **2(b)** complexes.

(ii) $n = 3$: When we add a new NH_3 molecule (NH_3(n)) to **2(a)** and **2(b)** structures, we obtain three stable optimized structures noted **3(a)**, **3(b)** and **3(c)**:

(1) The less stable structure **3(a)** (ΔE(BSSE) = −89.03 kJ/mol) corresponds to the addition of NH_3(n) on the H of NH_3(r) of the **2(b)** system. This new additional NH_3 presents a weak H-bond ($r_5 = 2.094$ Å in Figure 5) with the HNCO:$(NH_3)_2$ system. The previous H-bonds are altered: r_3 decreased to 2.366 Å and r_4 increased to 2.169 Å. This third NH_3 does not involve any interaction with HNCO. NH_3(n) contributes, by hyperconjugation, to the lengthening of r_1 to 1.088 Å and the shortening of r_2 to 1.617 Å, without interacting with HNCO.

(2) The second structure noted as **3(b)** corresponds to the interaction of NH_3(n) with the oxygen of HNCO in the previous **2(a)** and **2(b)** systems. This structure presents four H-bonds forming a quasiplanar cycle with the three NH_3. Its ΔE(BSSE) = −89.45 kJ/mol, very close to that of **3(a)** (ΔE = 0.42 kJ/mol). The H-bonds r_2 and r_4, 1.665 and 2.022 Å, respectively, decrease. A new H-bond, noted as r_3 in **3(b)**, is observed between the oxygen of HNCO and a hydrogen of NH_3(n) ($r_3 = 2.192$ Å). A NH_3 dimer interaction r_5, between the nitrogen of NH_3(n) and a hydrogen of a second NH_3, is 2.143 Å. As in **3(a)**, r_1 is lengthening to 1.064 Å and r_2 is shortening to 1.665 Å.

(3) The last structure **3(c)**, the most stable (ΔE(BSSE) = −90.70 kJ/mol), corresponds to the interaction of NH_3(n) with an H of NH_3(r) of **2(a)**. NH_3(n) presents an H-bond ($r_5 = 2.161$ Å) with NH_3(r) without interaction with HNCO. The two H-bonds (r_2 and r_3), correspond to the interaction of HNCO with NH_3(r) and the second NH_3. Their lengths are respectively 1.584 and 2.544 Å. The r_4 bond length increased to 2.153 Å (2.101 Å in **2(a)**) with the additional NH_3. As in **2(a)** and **2(b)**, r_1 increases, in this case to 1.088, 1.064, and 1.101 Å in **3(a)**, **3(b)**, and **3(c)**, respectively, and simultaneously r_2 decreases to 1.617, 1.665, and 1.584 Å.

(iii) $n = 4$: The NH_3(n) was added to the three different systems **3(a)**, **3(b)**, and **3(c).** We obtain three optimized structures noted **4(a)**, **4(b),** and **4(c)**.

(1) **4(a)** is the less stable structure (ΔE(BSSE) = −99.48 kJ/mol). It was obtained by addition of NH_3(n) on the oxygen of HNCO in the **3(b)** system. It presents a nonplanar cyclic shape. NH_3(n) integrates in the cycle of **3(b)** and the new system presents five hydrogen bonds (r_2, r_3, r_4, r_5, and r_6, with

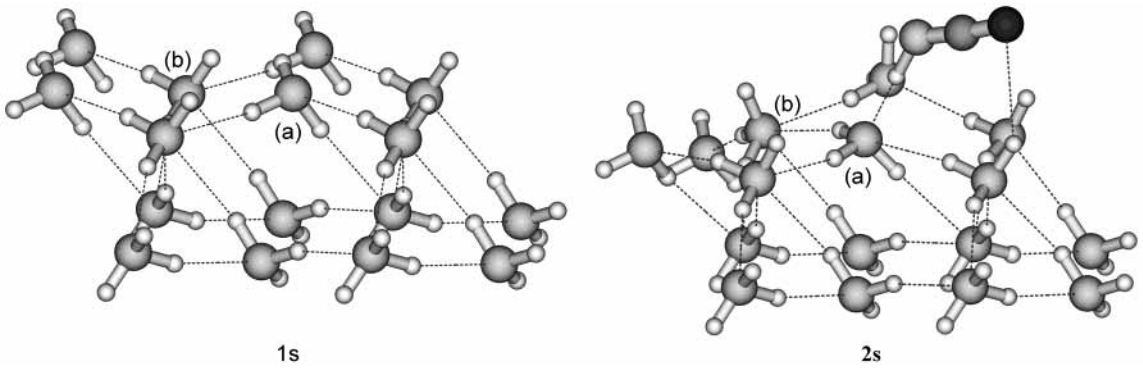

Figure 6. Surface of NH_3 (1s) and the whole system (surface + HNCO) (2s).

respectively 1.611, 2.208, 1.930, 2.014, and 2.136 Å). The NH length (r_1) of HNCO is 1.087 Å.

(2) When NH_3(n) is added on the oxygen of HNCO in **3(c)** or on a hydrogen of NH_3(r) in **3(b)**, the two systems yield spontaneously $[NH_4^+OCN^-](NH_3)_3$ and we obtain the **4(b)** structure. The formation of NH_4^+ and OCN^- ions is obtained by proton transfer from HNCO to NH_3(r) ($r_1 = 1.551$ Å). The new NH covalent bond is r_2 (1.070 Å) and the previous r_3, r_4, r_5, and r_6 bonds are modified to 2.003, 1.781, 1.979, and 1.930 Å, respectively. A new hydrogen bond (r_7), with a length of 2.170 Å, stabilizes OCN^-. In this structure, the isocyanate ion is stabilized by three H-bonds as observed with the dissociation of HNCO on water ice.[16] The ammonium ion exhibits three hydrogen bonds (r_1, r_4, and r_6), and only one hydrogen remains free of interaction. The interaction energy (ΔE(BSSE)) of this system is −375.30 kJ/mol.

(3) The last structure **4(c)** is the most stable (ΔE(BSSE) = −453.18 kJ/mol). As for **4(b)**, we have spontaneous formation of $[NH_4^+OCN^-](NH_3)_3$. This system is obtained by addition of NH_3(n) to the last H of NH_3(r) of the **3(a)** and **3(c)** system. The isocyanate ion displays three hydrogen bonds (r_1, r_3, and r_7 respectively 1.715, 2.046, and 2.137 Å). The different bonds of NH_4^+ are attached to three NH_3 molecules and OCN^- via hydrogen bonding. The lengths of the different H-bonds r_4, r_5, and r_6 between the NH_3 and NH_4^+ are 1.892, 1.952, and 1.945 Å.

Our results show that the stabilization effect of the system increases with the number of NH_3. The gain between every addition of NH_3 is about 20 kJ/mol from $n = 1$ to 4.[37] When $n = 3$, the total gain in energy is roughly equal to a covalent bond energy. As a consequence, for $n = 4$, the H−NCO bond breaking is completely offset by the bulk effect in **4(b)** and by the solvation contribution in **4(c)**. The resulting systems are energetically stable. These results are consistent with the calculations of Daigoku[37] and Wang.[38] Both found a stabilization effect of NH_4^+ with full solvation of NH bonds in a symmetry T_d for $NH_4^+(NH_3)_4$. The NH_4^+ bond lengths decrease continuously, while the hydrogen bond distances NH···N with the NH_3 solvents increase, from $NH_4^+(NH_3)$ to $NH_4^+(NH_3)_4$.[38] The different values obtained by Wang for $NH_4^+(NH_3)_3$ are in good agreement with our geometries for **4(b)** and **4(c)**, even if the symmetry is broken in our case.

Quantum calculations confirm the spontaneous character of the reaction between HNCO and NH_3 at 10 K. Due to the proton donor character of the HNCO molecule, we confirm that the ionization process occurs if one NH_3 molecule is in interaction with HNCO via its electron lone pair, and if this NH_3 is solvated enough. At least three NH_3 molecules are required to induce a spontaneous proton transfer.

TABLE 6: Wyckoff Optimized Coordinates (u, v, w) for Orthorhombic NH_3 Solid[a]

	u	v	w	u'	v'	w'
N_1	−0.05495	−0.04550	−0.03581	0.	0.	0.
N_2	0.55495	0.04550	0.46419	0.5	0.	0.5
N_3	0.05495	0.45450	0.53581	0.	0.5	0.5
N_4	0.44505	0.54550	0.03581	0.5	0.5	0.
H_1	−0.15076	0.01427	0.12533			
H_2	0.10251	−0.15455	0.01803			
H_3	0.00760	0.11788	−0.13448			
H_4	0.65076	−0.01427	0.62533			
H_5	0.39749	0.15455	0.51803			
H_6	0.49240	−0.11788	0.36552			
H_7	0.15076	0.51427	0.37467			
H_8	−0.10251	0.34545	0.48197			
H_9	−0.00760	0.61788	0.63448			
H_{10}	0.34924	0.48573	−0.12533			
H_{11}	0.60251	0.65455	−0.01803			
H_{12}	0.50760	0.38212	0.13448			

[a] Space group (no. 19) $P2_13$. Lattices constants: $a = 5.142$ Å, $b = 5.175$ Å, $c = 5.198$ Å, and $\beta = 90.0°$. For comparison, data corresponding to experimental structure are also reported, labeled (u', v', w') and $a' = b' = c' = 5.138$ Å

3.2. Surface Model and Adsorption NH_3 Ice. *3.2.1. Crystal Structure of Ammonia.* Ammonia is a compound whose crystal structure has received little attention. Ammonia and deuterioammonia have been studied by X-ray methods[28] and neutron diffraction,[39] respectively. Up to now experimental information about the structure of clean NH_3 ice surfaces on a molecular scale has been absent. Thus, as a first step before recognition of the adsorption mechanism, a theoretical study of the NH_3 surface has fundamental significance. Hence, one of the aims of our investigation is to formulate a reasonable and treatable model of the NH_3 surface. It is natural to approach this problem of surface through calculations on the solid ammonia.

The structure can be roughly described as slightly deviating from face centered cubic. There are four molecules in the cubic unit cell and the space group is $P2_13$.[28] The unit cell constants and the atomic coordinates were optimized by using the DFT formalism combined with a plane wave basis set. All calculations were done with the Castep code.[40] The gradient-corrected functional PW91[41] was used for exchange and correlation. We used nonlocal reciprocal-space pseudopotentials in the Kleinman−Bylander form.[42] The plane wave cutoff energy was 220 eV. The Brillouin zone was sampled by 4, 4, and 4 points following k_x, k_y, and k_z. After minimization, small deviation from the cubic symmetry was observed: NH_3 was found to be orthorhombic, but the three lattice parameters were very close to each other. We report the calculated atomic positions in Table 6.

3.2.2. Adsorption of HNCO on NH_3 Ice Surface. We have performed DFT calculations to consider adsorption of HNCO

on the (001) NH_3 surface. We have used a cluster model to represent the clean surface. The positions of the cluster atoms were initially fixed to those of solid NH_3. Calculations have been performed with ab initio DFT and Gaussian 98 code.[33] The whole system (surface + HNCO) was optimized without any restriction, taking into account the relaxation of the surface structure. The surface and the whole system are depicted in Figure 6, 1s and 2s. Advantages and limitations of the cluster model already have been discussed in other papers.[43,44]

After optimization, the adsorption energy was calculated to be −74.3 and −96.8 kJ/mol with and without BSSE corrections, respectively. The system stability is ensured by a strong hydrogen bond (1.662 Å) with a nearby N atom (noted N_a) of the surface. This hydrogen bond length formation is consistent with the perturbation on the dangling N−H adsorption in the IR spectrum. The oxygen of isocyanic acid interacts to a lesser extent with another neighboring NH group since the corresponding distance is 2.628 Å.

However, the adsorbate seems to be able to modify the surface structure. First, the $(NH_3)_a$ molecule tilts toward the surface, which leads to greater interaction between it and the $(NH_3)_b$ group: $[d\{(N-H)_a\cdots N_b\} = 2.40$ Å]. Second, in addition to this new weak $(N-H)_a-N_b$ bond, the $(NH_3)_a$ molecule manages to acquire a new $(N)_a\cdots$HNCO bond due to the strong availability of the lone pair orbital of the N_a atom, the angle $(OCN-H\cdots N_a)$ being 3°. In addition, there is no steric hindrance for the tilting of this $(NH_3)_a$ molecule on the surface.

After relaxation, the N−H bond length for the HNCO adsorbed molecule increases to 1.076 Å compared to the value of 1.008 Å for the free HNCO, which suggests a decrease of bond strength. Moreover, the charge distribution of the HNCO on the surface ($Q_{NCO} = -0.49$ au and $Q_H = 0.37$ au) indicates a charge transfer from HNCO to ammonia surface, in agreement with our former results.

A similar structure was also observed for the interaction of HNCO with amorphous water ice, before dissociation. In this case, the dissociation of the proton from the isocyanic acid occurs near 110 K, with an energy barrier estimated to 42 kJ/mol.[16] With solid ammonia, dissociation occurs near 90 K.

These theoretical results suggest that we are in a predissociation state. So, this model shows that the N−H bond of isocyanic acid should dissociate easily with the NH_3 surface to form the NH_4^+ species. Experimentally, the absorption band of the OCN^- species appears at 50 K with a crystalline ice surface of NH_3.

4. Conclusion

We showed that when HNCO is co-deposited with NH_3 in argon matrix at 10 K a predominant 1:1 hydrogen-bonded complex is formed in which HNCO displays a proton donor character. An annealing of the matrix at 10 K induced the formation of a new of complex, which is probably $HNCO(NH_3)_2$, and the formation of $NH_4^+OCN^-$. A co-deposition of pure HNCO and an excess of NH_3 at 10 K induces the spontaneous $NH_4^+OCN^-$ formation. The more typical vibration bands of $NH_4^+OCN^-$, which serve to probe its identification, at 2151 and 1495 cm^{-1} are in excellent agreement with the values reported for $NH_4^+OCN^-$ induced during the photolysis of CO/NH_3 ices.[29] The behavior of HNCO is different when it is adsorbed on NH_3 amorphous or crystal ice surface. In these conditions, no reaction occurs at 10 K, but only when the sample is warmed above 50 (for crystal NH_3 ice film) or 90 K (for amorphous NH_3 ice film).

The quantum calculations confirm the spontaneous character of the $NH_4^+OCN^-$ formation when HNCO is in an environment of four NH_3. The position of the four NH_3 in this environment plays an important role in the reaction. The ionization process occurs only if one NH_3, solvated at least by two other NH_3, is in interaction with the hydrogen of HNCO via its electron lone pair.

We believe that the nondetection of HNCO in solid in the interstellar grain, nevertheless produced in laboratory photolysis of $CO/NH_3/H_2O$ or CO/NH_3 mixtures,[45] can be due both to its great reactivity to NH_3 and to its fast photodecomposition.[46]

References and Notes

(1) Winnewisser, G.; Kramer, C. *Space Sci. Rev.* **1999**, *90*, 181.
(2) Charnley, S. B.; Ehrenfreund, P.; Juan, Y.-J. *Spectrochim. Acta, Part A* **2001**, *57*, 685.
(3) Bernstein, M. P.; Allamandola, L. J.; Sandford, S. A. *Adv. Space Res.* **1997**, *19*, 991.
(4) Soifer, B. T.; Puetter, R. C.; Russel, R. W.; Willner, S. P.; Harvey, P. M.; Gillet, F. C. *Astrophys. J.* **1979**, *232*, L53.
(5) Lacy, J. H.; Baas, F.; Allamandola, L. J.; Persson, S. E.; McGregor, P. J.; Londsdale, C. J.; Geballe, T. R.; Van de Bult, C. E. P. *Astrophys. J.* **1984**, *276*, 523.
(6) Larson, H. P.; David, D. S.; Black, J. H.; Frisk, *Astrophys. J.* **1985**, *299*, 873.
(7) d'Hendecourt, L.; Allamandola, L. J.; Grim, R. J. A.; Greenberg, J. M. *Astron. Astrophys.* **1986**, *158*, 119.
(8) Grim, R. J. A.; Greenberg, J. M. *Astrophys. J.* **1987**, *321*, L91.
(9) Schutte, W. A.; Greenberg, J. M. *Astron. Astrophys.* **1997**, *317*, L43.
(10) Demyk, K.; Dartois, E.; d'Hendecourt, L.; Jourdain de Muizon, M.; Heras, A. M.; Breitfeller, M. *Astron. Astrophys.* **1998**, *339*, 553.
(11) Bernstein, M. P.; Sandford, S. A.; Allamandola, L. J.; Chang, S.; Scharberg, M. A. *Astrophys. J.* **1995**, *454*, 327.
(12) Hudson, R. L.; Moore, M. H. *Astrophys. J.* **2000**, *357*, 787.
(13) Novozamsky, J. H.; Schutte, W. A.; Keane, J. V. *Astron. Astrophys.* **2001**, *379*, 588.
(14) Hudson, R. L.; Moore, M. H.; Gerakines, P. A. *Astrophys. J.* **2001**, *550*, 1140.
(15) (a) Van Dishoek, E. F.; Blake, G. A. *Annu. Rev. Astron. Astrophys.* **1998**, *36*, 317. (b) Turner, B. E.; Terzieva, R.; Herbst, E. *Astrophys. J.* **1999**, *518*, 699.
(16) Raunier, S.; Chiavassa, T.; Allouche, A.; Marinelli, F.; Aycard, J. P. *Chem. Phys.* **2003**, *288*, 197.
(17) Raunier, S.; Chiavassa, T.; Allouche, A.; Marinelli, F.; Aycard, J. P. *Chem. Phys. Lett.* **2003**, *368*, 594.
(18) Gibb, E. L.; Whittet, D. C. B.; Schutte, W. A.; Boogert, A. C. A.; Chiar, J. E.; Ehrenfreund, P.; Gerakines, P. A.; Keane, J. V.; Tielens, A. G. G. M.; van Dishoeck, E. F.; Kerkhif, O. *Astrophys. J.* **2000**, *536*, 347.
(19) Herzberg, G.; Reid, C. *Discuss. Faraday Soc.* **1950**, *9*, 92.
(20) Sheludyakov, Y. L.; Shubareva, F. Z.; Golodov, V. A. *J. Appl. Chem.* **1994**, *67*, 780.
(21) Pietri, N.; Jurca, B.; Monnier, M.; Hillebrand, M.; Aycard, J. P. *Spectrochim. Acta, Part A* **2000**, *56*, 157.
(22) (a) Sefik, S.; Lester, A. *J. Chem. Phys.* **1987**, *87*, 5131. (b) Nishiya, T.; Hirota, N.; Shirohara, H.; Nishi, N. *J. Phys. Chem.* **1985**, *89*, 2260. (c) Schimanouchi, T. In National Standard Reference Data System; U.S. Government Printing Office: Washington, DC, 1972; Vol. 39.
(23) Teles, J. H.; Maier, G.; Hess, B. A.; Schaad, L. J.; Winnewisser, M.; Winnewisser, B. P. *Chem. Ber.* **1991**, *122*, 753.
(24) Staats, P. A.; Morgan, H. W. *J. Chem. Phys.* **1959**, *31*, 553.
(25) Ferraro, J. R.; Sill, G.; Fink, U. *Appl. Spectrosc.* **1980**, *34*, 525.
(26) Pipes, J. G.; Roux, J. A.; Smith, A. M. *AIAA J.* **1978**, *16*, 984.
(27) Mantz, A. W.; Thomson, S. B.; Arnold, F.; Sanderson, R. B. In *Thermophysics and Spacecraft Thermal Control Progress in Astronautics and Aeronautics*: MIT Press: Cambridge, MA, 1974; Vol. 35, p 229.
(28) Olovsson, I.; Templeton, D. H. *Acta Crystallogr.* **1959**, *12*, 832.
(29) Lowenthal, M. S.; Khanna, R. K.; Moore, M. H. *Spectrochim. Acta, Part A* **2002**, *58*, 73.
(30) Wagner, E. L.; Hornig, D. F. *J. Chem. Phys.* **1950**, *18*, 296.
(31) Dunitz, J. D.; Harris, K. D. M.; Johnston, R. L.; Kariuki, B. M.; MacLean, E. J.; Psallidas, K.; Schweizer, W. B.; Tykwinski, R. R. *J. Am. Chem. Soc.* **1998**, *120*, 13274.
(32) Bernstein, M. P.; Sandford, S. A.; Allamandola, L. J. *Astrophys. J.* **2000**, *542*, 894.
(33) Frisch, M. J.; Trucks, G. W.; Schlegel, H. B.; Scuseria, G. E.; Robb, M. A.; Cheeseman, J. R.; Zakrzewski, V. G.; Montgomery, J. A., Jr.; Stratmann, R. E.; Burant, J. C.; Dapprich, S.; Millam, J. M.; Daniels, A. D.; Kudin, K. N.; Strain, M. C.; Farkas, O.; Tomasi, J.; Barone, V.; Cossi, M.; Cammi, R.; Mennucci, B.; Pomelli, C.; Adamo, C.; Clifford, S.;

Ochterski, J.; Petersson, G. A.; Ayala, P. Y.; Cui, Q.; Morokuma, K.; Malick, D. K.; Rabuck, A. D.; Raghavachari, K.; Foresman, J. B.; Cioslowski, J.; Ortiz, J. V.; Baboul, A. G.; Stefanov, B. B.; Liu, G.; Liashenko, A.; Piskorz, P.; Komaromi, I.; Gomperts, R.; Martin, R. L.; Fox, D. J.; Keith, T.; Al-Laham, M. A.; Peng, C. Y.; Nanayakkara, A.; Gonzalez, C.; Challacombe, M.; Gill, P. M. W.; Johnson, B.; Chen, W.; Wong, M. W.; Andres, J. L.; Gonzalez, C.; Head-Gordon, M.; Replogle, E. S.; Pople, J. A. *Gaussian 98*, Revision A.7; Gaussian, Inc.: Pittsburgh, PA, 1998.

(34) Parr, R. G.; Yang, W. In *Density-Functional Theory of Atoms and Molecules;* Oxford University Press: New York, 1989.

(35) Boys, S.; Bernardi, F. *Mol. Phys.* **1970**, *19*, 553.

(36) (a) Masella, M.; Flament, J.-P. *J. Chem. Phys.* **1999**, *110*, 7245. (b) Scheiner, S. In *Hydrogen Bonding*: *A Theoretical Perspective*; Oxford University Press: Oxford, UK, 1997.

(37) Daigoku, K.; Miura, N.; Hashimoto, K. *Chem. Phys. Lett.* **2001**, *346*, 81.

(38) Wang, B.-C.; Chang, J.-C.; Jiang, J.-C.; Lin, S.-H. *Chem. Phys.* **2002**, *276*, 93.

(39) Reed, J. W.; Harris, P. M. *J. Chem. Phys*. **1961**, *35*, 1730.

(40) Milman, V.; Winkler, B.; White, J.; Pickard, C.; Payne, M.; Akhmatskaya, E.; Nobes, R. *Int. J. Quantum Chem.* **2000**, *77*, 895.

(41) Perdew, J. P.; Wang, Y. *Phys. Rev. B* **1992**, *46*, 6671.

(42) Kleinman, L.; Bylander, D. M. *Phys. Rev. Lett.* **1982**, *48*, 1425.

(43) Martins, J. B. L.; Taft, C. A.; Longo, E.; Andres, J. *J. Mol. Struct. (THEOCHEM)* **1997**, *398*−*399*, 457.

(44) Pacchioni, G.; Ferrari, A. M.; Ierano, G. *Faraday Discuss.* **1997**, *106*, 155.

(45) Whittet, D. C. B.; Schutte, W. A.; Tielens, A. G. G. M.; Boogert, A. C. A.; de-Graauw, T.; Ehrenfreund, P.; Gerakines, P. A.; Helmich, F. P.; Prusti, T.; van-Dishoeck, E. F. *Astron. Astrophys.* **1996**, *315*, 357.

(46) Pettersson, M.; Khriachtchev, L.; Jolkkonen, S.; Räsänen, M. *J. Phys. Chem. A* **1999**, *103*, 9154.